BULETINUL INSTITUTULUI POLITEHNIC DIN IAŞI
Publicat de
Universitatea Tehnică „Gheorghe Asachi" din Iași
Volumul 71 (75), Numărul 1, 2025
Secţia
CONSTRUCŢII DE MAŞINI
DOI:10.2478/bipcm-2025-0001

KINEMATIC MODELING AND SIMULATION OF HAND MUSCLE STRENGTH REHABILITATION USING INTELLIGENT PNEUMATIC MECHANISMS

BY

CEZAR MUCILEANU[1], MARIANA ROTARIU[1,2] and IRINA DUDUCA[1,*]

[1]University of Medicine and Pharmacy "Grigore T. Popa" Iași, Faculty of Medical Bioengineering, Iași, Romania
[2]"Gheorghe Asachi" Technical University of Iași, Faculty of Machines Manufacturing and Industrial Management, Iași, Romania

Received: February 19, 2025
Accepted for publication: March 14, 2025

Abstract. The human hand, with its complex biomechanical structure, requires precise mechanical modelling for effective rehabilitation solutions. The proposed system integrates a therapeutic glove with individual pneumatic chambers for each finger, a force-sensing resistor for measuring grip strength, and a control unit based on Arduino Due. The mechanical model follows the Modified Denavit-Hartenberg (MDH) convention, describing finger joints as a multi-degree-of-freedom system. By utilizing pneumatic components, the device ensures smooth and adjustable joint mobilization, simulating the natural movement of the hand. The dynamic model, derived using the Euler-Lagrange equations, accounts for kinetic interactions and potential energy, allowing for a precise estimation of muscle strength. Experimental validation demonstrates the efficacy of the glove in restoring joint angles and muscle strength. The proposed method confirms that the developed system provides an efficient mechanical

---

*Corresponding author; *e-mail*: irinaduduca30@gmail.com

framework for adaptive rehabilitation, offering real-time feedback for therapeutic optimization.

Keywords: Biomechanical Modelling, Pneumatic Glove, Kinematic Analysis, Hand Rehabilitation, Muscle Strength.

1. Introduction

The specialized literature states that the hand is defined by an open kinematic chain, originating at the radiocarpal joint and extending to the distal interphalangeal joints. The synovial joints of the hand, due to their specific conformation and biomechanics, primarily allow rotational movements. Structurally, the individual bone components are considered mobile parts, and the joints between them are classified as kinematic pairs of different classes, depending on the number of degrees of freedom they allow (Vasdeki *et al*., 2024).

The human hand is characterized as the most flexible segment of the human body, possessing a unique structure (Narumi *et al*., 2022; Tran *et al*., 2021). Structurally, the hand integrates 27 bones, 30 joints, and 19 muscles that work simultaneously to facilitate fine and precise movements. Through its architecture, the distal segment of the upper limb serves as an example of form adapting to function, enabling movements of varying complexity. Consequently, the importance of its functionality is significantly heightened, as any dysfunction can lead to imbalances in performing daily activities.

In this study, a robotic glove was used as an alternative rehabilitation method, serving as a device with applications in medical rehabilitation. It was utilized both for testing mechanical functions and for alleviating the sequelae resulting from various pathologies affecting the hand and fingers (Rainbow *et al*., 2015; Lee *et al*., 2019).

The presented system is a complex and innovative tool designed to facilitate the rehabilitation and mechanical testing of hand function (Meng *et al*., 2021), combining pneumatic elements with data acquisition using sensors, as well as mathematical modelling and simulation. It consists of a therapy glove, a pressure sensor integrated into a ball, and a data processing unit based on the Arduino Due platform.

The therapy glove is a medical device designed to aid in the recovery of hand function (Shiqing *et al*., 2024). It is made of a flexible and comfortable material with an adjustable fastening system. The external control unit allows for the customization and monitoring of therapy, being powered both by an external source and a rechargeable battery.

The integrated pneumatic system consists of an air pump, tubes, conduits, valves, and pneumatic compartments. The air pump serves as the source of compressed air, supplying the device through flexible tubes and conduits that connect the pump to the glove. To tailor the treatment plan according to the affected segment, valves and regulators were used to adjust the airflow and, consequently, the pressure directed toward the glove's compartments, enabling the movement of each finger. The pneumatic compartments are air chambers positioned at each finger, mechanically acting on each interphalangeal joint to facilitate their flexion (Polygerinos *et al*., 2013).

For the collection of experimental data during the rehabilitation process, an FSR 402 sensor was used. This sensor is part of the Interlink Electronics FSR™ 400 series, featuring a round shape with a diameter of 18.28 mm. It belongs to the Force Sensing Resistor™ family, robust thick-film polymeric devices that exhibit a decrease in resistance as the force applied to the sensor surface increases (Interlink Electronics, 2022).

The created system is based on an Arduino Due development board, which features the Atmel SAM3X8E microcontroller with a 32-bit ARM Cortex-M3 processor. According to the manufacturer's specifications, this board is ideal for various applications, including data processing, motor control, and advanced robotics (Arduino, 2025).

Connecting the board to a power source enabled the acquisition and processing of signals. The sensor used was connected to an integrated power source on the board and to port A1, which is responsible for data transmission. Additionally, to maintain the integrity of the components and ensure a reliable signal, a 10 kΩ resistor was integrated into the circuit.

With this system, data representing the grip force exerted by the fingers was acquired, allowing for its processing to generate a relevant graph depicting the force action over time.

2. Kinematic Modelling and Simulation of the Hand

To simulate finger musculature, specialized literature was consulted, where various mathematical models are used and described to understand the mechanical process and the degrees of freedom of the finger joints.

The kinematic model of the hand consists of 19 bony structures (referred to in the literature as links), represented by 5 metacarpal bones and 14 phalanges, with 24 degrees of freedom (DoFs) modelled through joints. Due to mechanical differences in mobility and the number of bones involved, two distinct kinematic configurations were created for the thumb and the other four fingers. The thumb is modelled with 3 links and 4 joints, while the index, middle, ring, and little fingers are modelled with 4 links and 5 joints (Dragusanu *et al*., 2024).

Fai Chen Chen and his collaborators (Chen Chen *et al*., 2014) described in their study a mathematical model that analyses the direct kinematics of the four fingers, excluding the thumb. This model provides information on the position and orientation of the fingertip based on joint angles. The model's equations are calculated using the Modified Denavit-Hartenberg (MDH) parameters introduced by J.J. Craig (1986).

The four bones of each finger form a series of joints, namely: the Carpometacarpal (CMC) joint, the Metacarpophalangeal (MCP) joint, the Proximal Interphalangeal (PIP) joint, and the Distal Interphalangeal (DIP) joint. In terms of mobility, the CMC joint is responsible for hand deformation during object gripping, such as squeezing a ball used for muscle strength rehabilitation. The MCP joint has two degrees of freedom, allowing adduction-abduction and flexion-extension movements. The PIP and DIP joints permit only flexion and extension movements. In accordance with the representation in Fig. 1, the fingers are indexed using a numerical system from 0 to 4. This quantification scale assigns the value 0 to the thumb, while the values from 1 to 4 are sequentially allocated to the index, middle, ring, and little fingers, respectively.

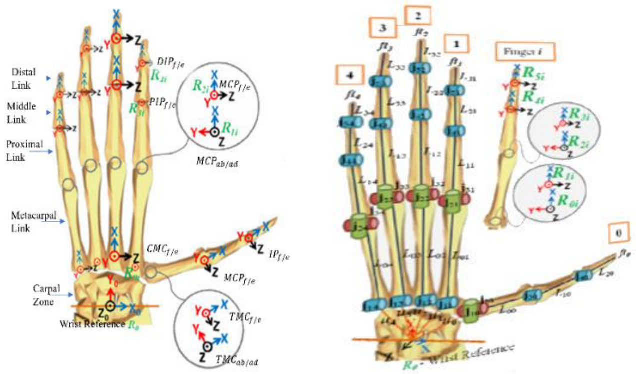

Fig. 1 – Kinematic configuration of the human hand (Chen Chen *et al*., 2013).

The equation Eq. (1) represents the forward kinematics of the index finger (i=1) up to the little finger (i=4) (Chen Chen *et al*., 2014):

$$Q_i = {}^0_0T_i \cdot {}^0_6T_i(\theta_j) = {}^0_0T_i \cdot \prod_{j=1}^{5} {}^{(j-1)}_{j}T_i(\theta_j) \cdot {}^5_6T_{ft_i} = {}^0_0T_i \cdot {}^0_1T_i\left(\theta_{CMC_{f/e}}\right) \cdot$$

$$\cdot {}^1_2T_i\left(\theta_{MCP_{ab/ad}}\right) \cdot {}^2_3T_i\left(\theta_{MCP_{f/e}}\right) \cdot {}^3_4T_i\left(\theta_{PIP_{f/e}}\right) \cdot {}^4_5T_i\left(\theta_{DIP_{f/e}}\right) \cdot {}^5_6T_{ft_i} \qquad (1)$$

Where:

- Q is a matrix that integrates the position and orientation of the fingertip for each finger;
- ${}^0_0T_i$ represents a roto-translation matrix that models the initial configuration of the fingers, considering their slightly divergent arrangement. This matrix allows the transition from the initial base reference system (R_0) to the alignment of the first reference system of finger i (R_{0i});

- ${}^{0}_{6}T_i(\theta_j)$ is a matrix that contains the geometric transformation between the first reference system of finger i and its fingertip (ft_i), the resulting matrix represents the composition of geometric transformations corresponding to each segment of the finger;
- ${}^{(j-1)}_{j}T_i(\theta_j)$ is a matrix that contains the geometric transformations between the *(j-1)* reference system and the j reference system of finger i;
- ${}^{5}_{6}T_{ft_i}$ represents the position of the fingertip relative to the distal reference system;
- j corresponds to each joint of the finger $CMC_{f/e}$, $MCP_{ab/ad}$, $MCP_{f/e}$, $PIP_{f/e}$, $DIP_{f/e}$;
- ft_i represents the fingertip i.

The results obtained from the specialized literature and used in the modelling process are described in Table 1.

Table 1
Modified Denavit-Hartenberg parameters (Chen Chen *et al*., 2014)

Joint	α_{i-1}	a_{i-1}	d_i	θ_i
j_{1i}	$\pi/2$	0	0	$\theta_{CMC_{f/e}}$
j_{2i}	$-\pi/2$	L_{01}	0	$\theta_{MCP_{ab/ad}}$
j_{3i}	$\pi/2$	0	0	$\theta_{MCP_{f/e}}$
j_{4i}	0	L_{11}	0	$\theta_{PIP_{f/e}}$
j_{5i}	0	L_{21}	0	$\theta_{DIP_{f/e}}$

The Euler-Lagrange equations allow for the dynamic modelling of a single finger (Fig. 2) using a set of mathematical equations. Since the metacarpal is considered fixed while the finger phalanges are the moving parts, R_2 has been established as the base reference system, and all equations are written relative to it.

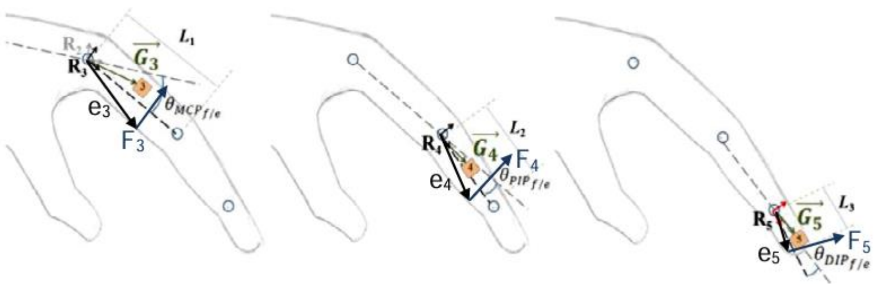

Fig. 2 – Dynamic model of a finger (Chen Chen *et al*., 2014).

The kinetic energy is calculated based on the position vectors of the centre of mass of each phalanx relative to the base reference system R_2. In general, the position of the centre of mass of phalanx j relative to its own reference system j is $G_j = [b_{jx} \quad b_{jy} \quad 0]^T$, where j=3,4,5. The mass of phalanx is m_j, and its corresponding moment of inertia about the *Oz* axis is I_j.

To solve the mathematical model and express it in its matrix form, the notations from Eq. (2) were used (Chen Chen *et al*., 2014):

$$\psi_3 = \theta_{MCP_{f/e}};\ \psi_4 = \theta_{MCP_{f/e}} + \theta_{PIP_{f/e}};\ \psi_5 = \theta_{MCP_{f/e}} + \theta_{PIP_{f/e}} + \theta_{DIP_{f/e}} \quad (2)$$

The generic position vector of the centre of mass relative to the base system R_2 is given by Eq. (3) (Chen Chen *et al*., 2014):

$$G_j = [G_{jx} \quad G_{jy} \quad G_{jz}]^T = \sum_{q=3}^{j-1} \begin{bmatrix} L_{q-2} c\psi_q \\ L_{q-2} s\psi_q \end{bmatrix} + \begin{bmatrix} b_{jx} c\psi_j - b_{jy} s\psi_j \\ b_{jx} s\psi_j + b_{jy} c\psi_j \\ 0 \end{bmatrix} \quad (3)$$

The velocity of the generic centre of mass is described by Eq. (4) (Chen Chen *et al*., 2014):

$$v_{G_j} = \sum_{q=3}^{j-1} \begin{bmatrix} -L_{q-2}\dot{\psi}_q s\psi_q \\ L_{q-2}\dot{\psi}_q c\psi_q \\ 0 \end{bmatrix} + \begin{bmatrix} -b_{jx}\dot{\psi}_j s\psi_j - b_{jy}\dot{\psi}_j c\psi_j \\ b_{jx}\dot{\psi}_j c\psi_j - b_{jy}\dot{\psi}_j s\psi_j \\ 0 \end{bmatrix} \quad (4)$$

The kinetic energy can be described as follows (Eq. (5)) (Chen Chen *et al*., 2014):

$$T = \frac{1}{2}\sum_{j=3}^{5} \left(m_j v_{G_j}^2 + I_j {\dot{\psi}_j}^2 \right) \quad (5)$$

The potential energy includes a gravitational term and an elastic term. The rigidity is considered a constant with an average value k_j, which varies with direction. The potential energy is expressed by Eq. (6) (Chen Chen *et al*., 2014):

$$U = \sum_{j=3}^{5} \left(m_j g G_{jy} + \frac{1}{2} k_j \left(\psi_j - \psi_{j-1}\right)^2 \right) \quad (6)$$

Also known as the Rayleigh dissipation function, the generalized velocity function is defined by the relation (Eq. (7)) (Chen Chen *et al*., 2014):

$$F = \sum_{j=3}^{5} \left(\frac{1}{2} \beta_j \left(\dot{\psi}_j - \dot{\psi}_{j-1} \right)^2 \right) \tag{7}$$

The damping constant β_j e represents the non-conservative contribution caused by muscle action in moving the finger. Non-conservative forces contributed less than 15% to the total force response during static displacement. The values β_3, β_4, β_5 correspond to the damping values for the MCP, PIP, and DIP joints, respectively. Under these conditions, the Euler-Lagrange equations become Eq. (8) (Chen Chen *et al.*, 2014):

$$\frac{d}{dt}\left(\frac{\partial (T-U)}{\partial \dot{\psi}_j}\right) - \frac{\partial (T-U)}{\partial \psi_j} + \frac{\partial F}{\partial \dot{\psi}_j} = \tau_j \tag{8}$$

Where *j*=3,4,5. The terms τ_j represent the forces applied by the muscles to actuate the phalanx, and they can be defined according to Eq. (9) (Chen Chen *et al.*, 2014):

$$\tau_j = \frac{\sum_{j=3}^{5} \delta W_j}{\delta \psi_j} \tag{9}$$

Where, δw_j represents the virtual work performed by the force applied to the system, allowing us to rewrite it as (Eq. (10)) (Chen Chen *et al.*, 2014):

$$\begin{gathered} \tau_j = \left(F_{jy} e_{jx} - F_{jx} e_{jy}\right) + \\ + \sum_{q=j+1}^{5} \begin{bmatrix} -L_{(j-2)} s\theta_j \\ L_{(j-2)} c\theta_j \\ 0 \end{bmatrix} \cdot \begin{bmatrix} F_{qx} c\psi_q - F_{qy} s\psi_q \\ F_{qx} s\psi_q - F_{qy} c\psi_q \\ 0 \end{bmatrix} + C_{mj} - C_{m(j+1)} \end{gathered} \tag{10}$$

C_{mj} represents the torque produced by the muscles on joint *j* and $F_j = [F_{jx} \quad F_{jy} \quad 0]^T$ is the contact force applied to phalanx *j* at the point defined by the position vector $e_j = [e_{jx} \quad e_{jy} \quad 0]^T$. After calculating each term of the Euler-Lagrange equations, the matrix form of the dynamic system is obtained as Eq. (8) (Chen Chen *et al.*, 2014).

$$[A] \cdot [\ddot{\psi}_3 \quad \ddot{\psi}_4 \quad \ddot{\psi}_5]^T = [B] \tag{11}$$

Matrix *A* contains the coefficients of the accelerations, while vector *B* includes the remaining terms. Equation (Eq. 11) allows the calculation of finger movement, given the muscular torques applied to each phalanx.

3. Results and Discussion

With the developed system, Fig. 3 (a), (b), data collection is carried out for analysis to identify pressure patterns, variations in applied forces, and potential motor deficits observed during gripping exercises. Additionally, the results are analysed in the context of their clinical applicability, highlighting the relevance of using this system for hand grip strength testing to adapt the rehabilitation program.

Fig. 3 (a), (b) – The Developed System for Experimental Data Collection Using the Pneumatic Glove.

To perform these movements, the pneumatic glove was used to facilitate the passive mobilization of all finger joints with the aid of adjustable airflow (Fig. 4 (a), (b)).

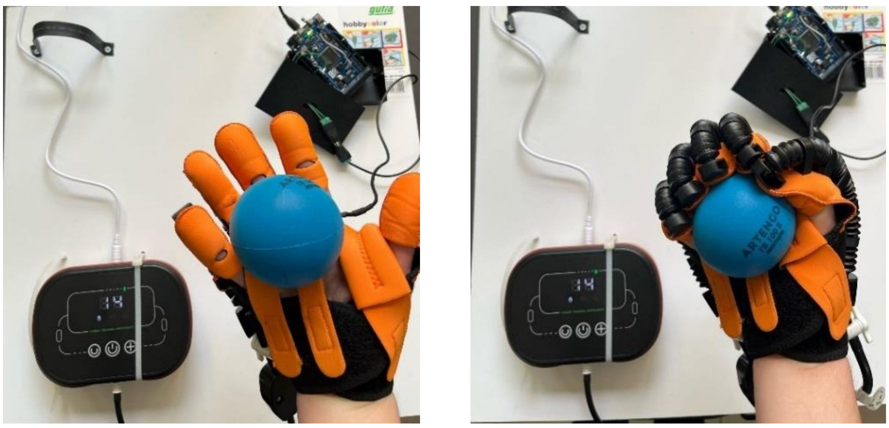

Fig. 4 (a), (b) – Example of the Functionality of the Hardware Component.

The graphs below provide a visualization of the data collected through the data acquisition system, representing variations in biomechanical parameters during the use of the proposed device. The graphical display was performed using the MATLAB platform, which served as the therapist-patient interface. The measurements were conducted in real-time, without data storage, during specific motor tasks such as rhythmic ball squeezing or applying pressure through the pneumatic system. The Ox-axis represents the evolution of the measurements over time (s), while the Oy-axis indicates the pressure level during testing (Kgf).

To highlight the functionality of the system, it was tested on three different patients (Fig. 5, Fig. 6, Fig. 7) in terms of age, sex, and degree of joint impairment.

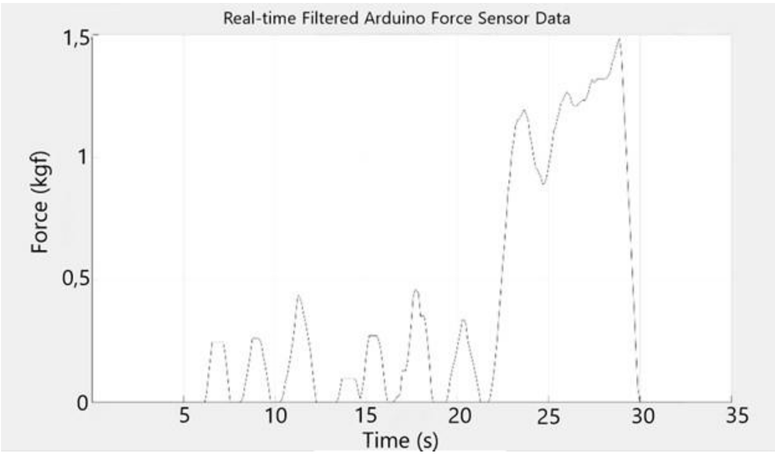

Fig. 5 – The collection of data from patient 1.

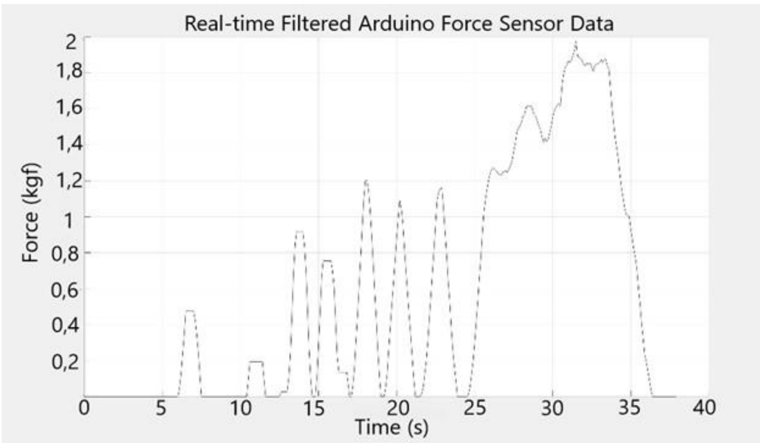

Fig. 6 – The collection of data from patient 2.

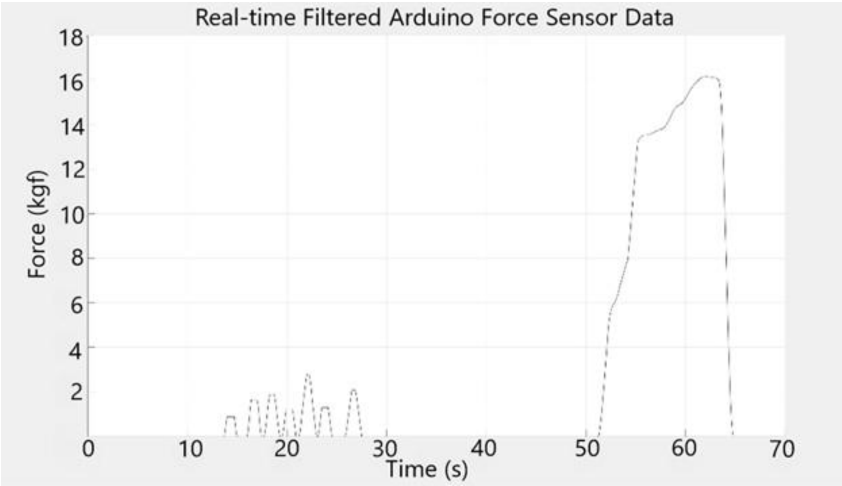

Fig. 7 – The collection of data from patient 3.

In this case, the patients are instructed to perform seven rhythmic ball squeezes, represented in the graph by the first seven peaks. Each peak corresponds to a phase of maximum contraction, followed by complete relaxation. The final contraction depicted in the graph consists of a passive ball squeeze assisted by the pneumatic glove. Passive squeezing refers to the action of gripping the ball without the active involvement of the patient's flexor muscles, being induced by an external factor, in this case, the pneumatic glove, which applies a controlled force to facilitate the gripping motion.

Analysing the results obtained from the three patients (Fig. 5, Fig. 6, Fig. 7), a difference in passive grip strength is observed, attributed to joint stiffness and the limited range of motion present at the level of the finger joints.

Following the completion of the tests, it was found that the first two patients (Fig. 5, Fig. 6) struggle to reach a passive grip force of 2 Kgf, whereas the third patient (Fig. 7) exceeds the threshold of 16 Kgf. The latter is considered the reference patient, as the obtained value falls within the normal physiological ranges, thus serving as a benchmark for assessing the performance and recovery level of the other patients.

4. Conclusions

By integrating biomechanical techniques with the pneumatic system and data processing, this rehabilitation device for muscle strength and finger and hand range of motion serves as an efficient tool for both evaluation and recovery. With the help of the microcontroller and force sensor, the device ensures real-time monitoring of the patient without storing data in memory, thus facilitating the rehabilitation process.

A possible research direction can be developed by storing the previously collected data, which will enable continuous monitoring of the patient's progress and the generation of reports on the recovery process.

These reports are highly valuable for objectively assessing the effectiveness of therapy, as they enable direct comparisons between different rehabilitation sessions and highlight the progress made. This type of objective evaluation is crucial in treatment planning, providing essential insights into what is effective and what requires adjustments.

REFERENCES

Arduino, *Product Reference Manual*, Retrieved 2025, (2025), https://docs.arduino.cc/resources/datasheets/A000062-datasheet.pdf.

Chen Chen F., Appendino S., Alain Favetto B., *Human Finger Kinematics and Dynamics*, In New Advances in Mechanisms, Transmissions and Applications, Springer Netherlands, 2014, 115-122.

Chen Chen F., Appendino S., Battezzato A., Favetto A., Mousavi M., Pescarmona F., *Constraint Study for a Hand Exoskeleton: Human Hand Kinematics and Dynamics*, Journal of Robotics (2013).

Craig J.J., *Introduction to Robotics, Mechanics and Control*, Pearson Education International, 67-76 (1986).

Dragusanu M., Troisi D., Suthar B., Hussain I., Prattichizzo D., Malvezzi M., *MGlove-TS: A modular soft glove based on twisted string actuators and flexible structures*, Mechatronics (2024).

Interlink Electronics (2022), *FSR 402 Data Sheet.* Retrieved 2025, from https://www.interlinkelectronics.com/fsr-402.

Lee J.S., Kim Y.H., *Factors associated with limited hand motion after hand trauma,* Medicine, 98(3) (2019).

Meng Q., Shen Z., Nie Z., *Modeling and Evaluation of a Novel Hybrid-Driven Compliant Hand Exoskeleton Based on Human-Machine Coupling Model*, Applied Sciences, 11 (2021).

Narumi S., Huang X., Lee J., Kambara H., Kang Y., Shin D., *A Design of Biomimetic Prosthetic Hand*, Actuators, 11(6), 167 (2022).

Polygerinos P., Lyne S., Wang Z., Nicolini L.F., *Towards a Soft Pneumatic Glove for Hand* Rehabilitation, International Conference on Intelligent Robots and Systems (IROS), November 3-7, 2013, Tokyo, Japan, 1512-1517.

Rainbow M.J., Wolff A.L., Crisco J.J., Wolfe S.W., *Functional kinematics of the wrist*, The Journal of Hand Surgery (European Volume), 1(15) (2015).

Shiqing L., Chaofu L., Hui J., Yutao C., Yiqing X., Peng Y., Xia, H., *Finger Multi-Joint Trajectory Measurement and Kinematics Analysis Based on Machine Vision*, Actuators, 13(9), 332 (2024).

Tran P., Jeong S., Herrin K.R., Desai J.P., *Review: Hand Exoskeleton Systems, Clinical Rehabilitation Practices, and Future Prospects*, IEEE Transactions on Medical Robotics and Bionics, 3(3), 606-622 (2021).

Vasdeki D., Barmpitsioti A., De Leo A., Dailiana Z., *How to prevent hand injuries-Review of epidemiological data is the first step in health care management*, Injury, 55(3) (2024).

MODELAREA ȘI SIMULAREA CINEMATICĂ A REABILITĂRII FORȚEI MUSCULARE A MÂINII FOLOSIND MECANISME PNEUMATICE INTELIGENTE

(Rezumat)

Funcţionalitatea mâinii este esențială în activitățile zilnice, iar afecţiunile articulare sau traumatismele pot afecta semnificativ mobilitatea și forța musculară. Această lucrare prezintă dezvoltarea unui sistem robotic pentru reabilitarea mâinilor, bazat pe o mănușă pneumatică. Dispozitivul este alcătuit dintr-o mănușă terapeutică cu compartimente pneumatice individuale pentru fiecare deget, un senzor de presiune integrat într-o minge de testare și o unitate de procesare bazată pe Arduino Due.

Modelarea cinematică și dinamică a sistemului este realizat utilizând parametrii Denavit-Hartenberg modificați (MDH) și ecuațiile Euler-Lagrange, oferind o descriere detaliată a mișcării articulare și a forțelor implicate. Mănușa acționează mecanic asupra articulațiilor interfalangiene prin control pneumatic, facilitând atât mobilizarea pasivă a degetelor, cât și exercițiile active pentru recuperarea forței de prehensiune.

Sistemul a fost testat prin aplicarea și analiza datelor privind variația forței de prindere și amplitudinea mișcărilor, evidențiind un progres semnificativ în recuperare.